

Some models containing Regge poles*

3.1 Introduction

In the previous chapter we showed how, by analytically continuing the partial-wave amplitudes in angular momentum, one can represent the scattering amplitude as a sum of pole and cut contributions in the complex l plane. Cuts do not occur in potential scattering, or in some of the simpler models for strong interactions, and they will not be introduced until chapter 8. But Regge poles correspond to bound-state or resonance particles, and in this chapter we shall examine their occurrence in non-relativistic potential-scattering amplitudes, in Feynman perturbation field theory, and in various models of strong-interaction dynamics.

Though clearly none of these examples can prove that Regge poles will actually occur in hadronic processes, they do help to make it plausible. They also give some indication of the properties which Regge trajectories may be expected to possess.

We begin by discussing some of the more general results which are independent of particular models.

3.2 Properties of Regge trajectories

The analyticity and unitarity properties of the partial-wave amplitudes imply certain general features of the Regge trajectories.

For example the occurrence of a pole at $l = \alpha(t)$ implies that

$$(B_l(t))^{-1} \rightarrow 0 \quad \text{as} \quad l \rightarrow \alpha(t) \quad (3.2.1)$$

which may be used implicitly to define the function $\alpha(t)$, and hence tells us about the analyticity of $\alpha(t)$. It is more useful however to begin by writing, from (2.6.2) and (2.6.8) (Oehme and Tiktopoulos

* This chapter may be omitted at first reading.

1962, Barut and Zwanziger 1962),

$$\begin{aligned}
 B_l(t) &= \int_{s_T}^{s_1} + \int_{s_1}^{\infty} \left[\frac{1}{16\pi^2} Q_l(z_t) D_s(s, t) dz_t (q_{t13} q_{t24})^{-1} \right] \\
 &\equiv E_l(t) + F_l(t)
 \end{aligned}
 \tag{3.2.2}$$

where to define $E_l(t)$ and $F_l(t)$ we have split the region of integration at some arbitrary point s_1 . Then if $D_s(s, t) \sim s^{\alpha(t)}$, since from (A.27)

$$Q_l(z_t) \sim s^{-l-1}$$

we find that
$$F_l(t) \sim \int_{s_1}^{\infty} s^{-l-1+\alpha(t)} ds = -\frac{e^{(\alpha(t)-l)\log s_1}}{\alpha(t)-l} \tag{3.2.3}$$

and so contains the pole. $E_l(t)$ involves only a finite integration in s and so has no pole. Thus instead of (3.2.1) we can define $\alpha(t)$ by

$$(F_l(t))^{-1} \rightarrow 0 \quad \text{as } l \rightarrow \alpha(t) \tag{3.2.4}$$

It is evident from (3.2.2) that $F_l(t)$ has similar singularities to $B_l(t)$, i.e. the same dynamical right-hand cut starting at the threshold t_T , and a similar left-hand cut due to the s -singularities, but with the branch point pushed further to the left in the t plane as its position is determined by s_1 not s_T (substituted for M^2 in (2.6.16), see section 2.6). The kinematical threshold singularity has of course been removed from $B_l(t)$, and hence $F_l(t)$ in (3.2.2).

The implicit function theorem (Titchmarsh (1939) p. 198) tells us that if $(F_l(t))^{-1}$ is regular in the neighbourhood of some point $t = t_p$, say, and if

$$\frac{\partial}{\partial l} (F_l(t_p))^{-1} \Big|_{l=\alpha(t_p)} \neq 0 \tag{3.2.5}$$

then $\alpha(t_p)$ is also a regular function in the neighbourhood of t_p . This is easily demonstrated by expanding $(F_l(t_p))^{-1}$ in a Taylor series about $t = t_p$. $l = \alpha(t_p)$, i.e.

$$\begin{aligned}
 (F_l(t))^{-1} &= a_1(l - \alpha(t_p)) + a_2(l - \alpha(t_p))^2 + \dots + b_1(t - t_p) \\
 &\quad + b_2(t - t_p)^2 + \dots + c_2(t - t_p)(l - \alpha(t_p)) + \dots
 \end{aligned}
 \tag{3.2.6}$$

Then setting $(F_l(t))^{-1} = 0$ at $l = \alpha(t)$ gives

$$\alpha(t) = \alpha(t_p) - \frac{b_1}{a_1} (t - t_p) + \dots \tag{3.2.7}$$

a Taylor series for $\alpha(t)$, so α must be regular in the neighbourhood of t_p . However, if (3.2.5) does not hold, i.e. if $a_1 = 0$, then

$$\alpha(t) = \alpha(t_p) \pm \left(-\frac{b_1}{a_2} \right)^{\frac{1}{2}} (t - t_p)^{\frac{1}{2}} + \dots \tag{3.2.8}$$

and so there are two trajectories which cross at $t = t_p$, each with a square-root branch point, such that their imaginary parts for $t < t_p$ are equal and opposite, to preserve the analyticity of F_l^{-1} . Of course if b_1 also vanishes at this point there will not be a branch point.

Thus we conclude that $\alpha(t)$ will be analytic where F_l^{-1} is analytic unless two (or more) trajectories cross each other, in which case there may, but need not, be a branch point in each trajectory function. So unless trajectories cross we can expect $\alpha(t)$ to have the same singularities as $(F_l(t))^{-1}$. However, the position of the left-hand cut in $F_l(t)$ is arbitrary as it depends on s_1 . We can make s_1 as large as we like and still obtain a pole in (3.2.3) from the divergence of the integrand in (3.2.2) as $s \rightarrow \infty$, so it is evident that $\alpha(t)$ cannot contain the left-hand cut of $(F_l(t))^{-1}$. Hence $\alpha(t)$ has just the dynamical right-hand cut from $t_T \rightarrow \infty$, unless two trajectories collide.

Such collisions must in fact occur at $t = 0$ for fermion trajectories in order to satisfy the generalized MacDowell symmetry (see section 6.5 below). Also they have been observed to occur in various potential-scattering calculations, but this can only happen for $\text{Re}\{l\} < -\frac{1}{2}$ (see the next section). There is no direct evidence that complex trajectories occur in hadron physics for $t < 0$ (see however section 8.6), and it is usually assumed that the trajectory functions are real for $t < t_T$.

Then since $\alpha(t)$ is real analytic we can write a dispersion relation

$$\alpha(t) = \frac{1}{\pi} \int_{t_T}^{\infty} \frac{\text{Im}\{\alpha(t')\}}{t' - t} dt' \quad (3.2.9)$$

However, subtractions will usually be needed. For example if

$$\text{Re}\{\alpha(t)\} \xrightarrow{t \rightarrow \infty} A(t),$$

a polynomial in t , we may have

$$\alpha(t) = A(t) + \frac{1}{\pi} \int_{t_T}^{\infty} \frac{\text{Im}\{\alpha(t')\}}{t' - t} dt' \quad (3.2.10)$$

We shall find in the next section that with well behaved potentials like the Yukawa the trajectories tend to negative integers as $t \rightarrow \infty$, giving

$$\alpha(t) = -n + \frac{1}{\pi} \int_{t_T}^{\infty} \frac{\text{Im}\{\alpha(t')\}}{t' - t} dt', \quad n = 1, 2, 3, \dots \quad (3.2.11)$$

On the other hand in particle physics trajectories seem to be approximately linear, with rather small imaginary parts (see section 5.3) suggesting instead

$$\alpha(t) = \alpha_0 + \alpha_1 t + \frac{1}{\pi} \int_{t_T}^{\infty} \frac{\text{Im}\{\alpha(t')\}}{t' - t} dt' \quad (3.2.12)$$

Or the integral in (3.2.12) may not converge, in which case subtractions will be needed as in (1.10.10), and if for example two subtractions are sufficient we get

$$\alpha(t) = \alpha_0 + \alpha_1 t + \frac{t^2}{\pi} \int_{t_T}^{\infty} \frac{\text{Im} \{ \alpha(t') \}}{t'^2(t' - t)} dt' \tag{3.2.13}$$

We have chosen to make the subtractions at $t = 0$ so that $\alpha_0 = \alpha(0)$ and $\alpha_1 = \alpha'(0) \equiv (d\alpha/dt)_{t=0}$.

We shall find (see section 5.4) that $\text{Im} \{ \alpha(t) \} > 0$ for $t > t_T$, so if we take the n th derivative of (3.2.11) or (3.2.12) or (3.2.13)

$$\frac{d^n \alpha}{dt^n} = \frac{n!}{\pi} \int_{t_T}^{\infty} \frac{\text{Im} \{ \alpha(t') \}}{(t' - t)^{n+1}} dt' \tag{3.2.14}$$

we find that all the derivatives are positive for $t < t_T$. A function with this property is called a Herglotz function (Herglotz 1911).

If the pole takes the form (2.8.3), we have from (2.6.8)

$$B_l(t) \xrightarrow{l \rightarrow \alpha(t)} \frac{\gamma(t)}{l - \alpha(t)} \quad \text{where} \quad \gamma(t) \equiv \beta(t) (q_{t13} q_{t24})^{-\alpha(t)} \tag{3.2.15}$$

The function $\gamma(t)$, the Regge residue with the threshold behaviour removed, is often referred to as the ‘reduced residue’. We can use Cauchy’s residue theorem to write (from (3.2.2))

$$\gamma(t) = \frac{1}{2\pi i} \oint dl F_l(t) \tag{3.2.16}$$

where the integration contour is a closed path encircling the point $l = \alpha(t)$, but no other singularities of F_l . This equation together with the implicit function theorem tells us that $\gamma(t)$ will have similar analyticity properties to $\alpha(t)$, i.e. just the dynamical right-hand cut of $F_l(t)$ unless two or more trajectories cross. So as with (3.2.9) we can write

$$\gamma(t) = \frac{1}{\pi} \int_{t_T}^{\infty} \frac{\text{Im} \{ \gamma(t') \}}{t' - t} dt' \tag{3.2.17}$$

again making subtractions if necessary.

It is also possible to deduce the nature of the branch point in the trajectory function at t_T from the unitarity equation. If we consider the elastic scattering process $1 + 3 \rightarrow 1 + 3$ below the inelastic threshold in the t channel, t_I , we have, from (2.6.23),

$$\text{Im} \{ (B_l(t))^{-1} \} = -\rho(t) (q_{t13})^{2l}, \quad t_T < t < t_I \tag{3.2.18}$$

where $\rho(t) \equiv 2q_{t_{13}}t^{-\frac{1}{2}}$. Now the function

$$-\frac{i\rho(t)(-q_{t_{13}})^{2l}}{\cos \pi l} = -\frac{i\rho(t)(q_{t_{13}})^{2l}e^{\pm i\pi l}}{\cos \pi l} \tag{3.2.19}$$

has the same discontinuity as $(B_l(t))^{-1}$ for $t_T < t < t_1$, so that

$$Y(t, l) \equiv \cos \pi l (B_l(t))^{-1} + i\rho(t)(-q_{t_{13}})^{2l} \tag{3.2.20}$$

is analytic in this region. From (3.2.1.) we have

$$Y(t, l) \rightarrow i\rho(t)(-q_{t_{13}})^{2l}, \text{ for } l \rightarrow \alpha(t) \tag{3.2.21}$$

If we define $\alpha_T \equiv \alpha(t_T)$ we have (using (1.7.15), $t_T = (m_1 + m_3)^2$)

$$Y(t, \alpha_T) \approx -\frac{2}{\sqrt{t_T}} \left(\frac{t - t_T}{4}\right)^{\alpha_T + \frac{1}{2}} \text{ for } t \rightarrow t_T \tag{3.2.22}$$

so $Y(t_T, \alpha_T) = 0$ if $\alpha_T > -\frac{1}{2}$. We can expand Y in a Taylor series about the threshold values of t and α , giving

$$Y(t, \alpha(t)) = Y(t_T, \alpha_T) + Y'_l(\alpha(t) - \alpha_T) + Y'_l(t - t_T) + \dots \tag{3.2.23}$$

where

$$Y'_l \equiv \frac{\partial Y}{\partial l} \Big|_{l=\alpha_T}, \quad Y'_t \equiv \frac{\partial Y}{\partial t} \Big|_{t=t_T} \tag{3.2.24}$$

and so

$$\alpha(t) = \alpha_T - \frac{2}{\sqrt{t_T}} Y'_{l-1} \left(\frac{t - t_T}{4}\right)^{\alpha_T + \frac{1}{2}} e^{-i\pi(\alpha_T + \frac{1}{2})} - (t - t_T) \left(\frac{Y'_t}{Y'_l}\right) + \dots, \quad \alpha_T > -\frac{1}{2} \tag{3.2.25}$$

Hence the trajectory has a threshold cusp for $-\frac{1}{2} < \alpha_T < \frac{1}{2}$ and above threshold

$$\text{Im} \{\alpha(t)\} \sim (t - t_T)^{\alpha + \frac{1}{2}}, \quad t \approx t_T \tag{3.2.26}$$

However in potential scattering these cusp effects seem to be small (Warburton 1964).

Since

$$Y(t, l) \rightarrow -\frac{2}{\sqrt{t_T}}, \quad l \rightarrow -\frac{1}{2}, \quad t \rightarrow t_T, \tag{3.2.27}$$

the condition for a pole (3.2.1) becomes, from (3.2.20),

$$\frac{2}{\sqrt{t_T}} = \frac{2}{\sqrt{t_T}} (q_{t_{13}})^{2(l+\frac{1}{2})} e^{-i\pi(l+\frac{1}{2})} \tag{3.2.28}$$

which can be satisfied by $l = \alpha_n$ for any α_n such that

$$(\log(q_{t_{13}}^2) - i\pi)(\alpha_n + \frac{1}{2}) = 2\pi ni, \quad n = 0, \pm 1, \pm 2, \dots \tag{3.2.29}$$

that is

$$\alpha_n = \frac{2\pi n}{\pi + i \log(q_{t_{13}}^2)} - \frac{1}{2} \tag{3.2.30}$$

So an infinite number of trajectories converge on $\alpha = -\frac{1}{2}$ as $t \rightarrow t_T$ ($q_{t13} \rightarrow 0$). This is sometimes called the Gribov–Pomeranchuk phenomenon (Gribov and Pomeranchuk 1962). Their occurrence should serve as a warning against supposing that the left-half angular-momentum plane is likely to have a simple singularity structure.

3.3 Potential scattering

In this section we shall briefly review the behaviour of solutions of the Schroedinger equation for non-relativistic potential scattering as a function of l . As we have already mentioned this is how Regge poles were first discovered (Regge 1959) and there is the great advantage that all the results can be proved rigorously. But as potential scattering is only of limited relevance to particle physics our discussion will be rather cursory, and we refer the interested reader to more complete studies, where the required proofs are given in detail (Squires 1963, Newton 1964, de Alfaro and Regge 1965).

a. Solutions of the Schroedinger equation

If the interaction potential $V(r)$ is a function of the r only, the solutions of the Schroedinger equation (1.13.3)

$$\nabla^2\psi - U(r)\psi + k^2\psi = 0 \tag{3.3.1}$$

can be decomposed into partial waves (see for example Schiff (1968) p. 81)

$$\psi(r, \theta, \phi) = \sum_{l=0}^{\infty} \frac{1}{r} \phi_l(r) P_l(\cos \theta) \tag{3.3.2}$$

The cylindrical symmetry removes any dependence on the azimuthal angle ϕ , and the radial wave function $\phi_l(r)$ satisfies the radial Schroedinger equation (2.1.1)

$$\frac{d^2\phi_l(r)}{dr^2} + \left(k^2 - \frac{l(l+1)}{r^2} - U(r) \right) \phi_l(r) = 0 \tag{3.3.3}$$

The quantization of angular momentum, which restricts l to integer values, stems from the requirement that angular dependence of (3.3.2) be finite for all values of θ . But in (3.3.3) l appears as a free parameter, and the equation can be solved for any value of l . Poincaré’s theorem (see below) tells us that the solutions of such a differential equation are usually analytic functions of such parameters,

so we may expect $\phi_l(r)$ to be analytic in l . It is also useful to note the symmetry of (3.3.3) under the replacements $l \rightarrow -(l+1)$, and $k \rightarrow -k$.

As long as the potential is ‘regular’, i.e. $r^2U(r) \rightarrow 0$ as $r \rightarrow 0$, the small- r solutions of (3.3.3) are controlled by the centrifugal barrier term $l(l+1)r^{-2}$. This constitutes a repulsive addition to the effective potential (for $l > 0$), and physically of course it represents the increased difficulty of holding particles together if they have a high relative angular momentum due to the centrifugal force. As $r \rightarrow 0$ we can neglect k^2 and U in (3.3.3). Evidently there are two independent solutions which behave like r^{-l} and r^{l+1} , respectively, as $r \rightarrow 0$. The physical solution must be finite at the origin, however, and we denote it by $\phi_l(r) = \phi(l, k, r) \sim r^{l+1}$.

It satisfies the integral equation (Newton (1964) p. 21, de Alfaro and Regge (1965), p. 21)

$$\phi(l, k, r) = \phi_0(l, k, r) + \int_0^r dr' G(r, r') U(r') \phi(l, k, r') \quad (3.3.4)$$

where G is the Green’s function, which may be written in terms of Hankel functions as

$$G(r, r') = i \frac{\pi}{4} (rr')^{\frac{1}{2}} (H_{l+\frac{1}{2}}^{(2)}(kr) H_{l+\frac{1}{2}}^{(1)}(kr') - H_{l+\frac{1}{2}}^{(1)}(kr) H_{l+\frac{1}{2}}^{(2)}(kr')) \quad (3.3.5)$$

and where ϕ_0 is a solution of (3.3.3) with $U(r) = 0$, i.e.

$$\phi_0(l, k, r) = r^{\frac{1}{2}} \Gamma(l + \frac{3}{2}) \left(\frac{k}{2}\right)^{-l-\frac{1}{2}} J_{l+\frac{1}{2}}(kr) \quad (3.3.6)$$

J being a Bessel function. It can be checked by direct substitution that (3.3.4) satisfies (3.3.3), and the boundary condition at $r = 0$.

As long as $rU(r) \rightarrow 0$ as $r \rightarrow \infty$, both $U(r)$ and the centrifugal barrier term become irrelevant in (3.3.3) as $r \rightarrow \infty$, and in this limit it is more convenient to consider the ‘irregular’ solutions $\chi(l, \pm k, r)$ whose boundary conditions are $\chi(l, \pm k, r) \sim e^{\mp ikr}$ as $r \rightarrow \infty$, because these give the incoming and outgoing plane waves, in terms of which the scattering amplitude is defined. They satisfy the integral equation (Newton (1964) p. 14, de Alfaro and Regge (1965) p. 23)

$$\chi(l, k, r) = \chi_0(l, k, r) - \int_r^\infty G(r, r') U(r') \chi(l, k, r') dr' \quad (3.3.7)$$

where again G is given by (3.3.5) and χ_0 is a solution of (3.3.3) with $U(r) = 0$, i.e.

$$\chi_0(l, k, r) = e^{-i\frac{1}{2}\pi(l+1)} \left(\frac{\pi kr}{2}\right)^{\frac{1}{2}} H_{l+\frac{1}{2}}^{(2)}(kr) \tag{3.3.8}$$

The other independent solution is obtained by letting $k \rightarrow -k$.

Since any solution of (3.3.3) can be expressed in terms of these independent solutions, we can relate the physical solution (3.3.4) to the asymptotic plane-wave solutions (3.3.7), viz.

$$\phi(l, k, r) = \frac{1}{2ik} (f(l, k) \chi(l, -k, r) - f(l, -k) \chi(l, k, r)) \tag{3.3.9}$$

where the f 's are called Jost functions and satisfy (de Alfaro and Regge (1965) p. 39)

$$f(l, k) = f_0(l, k) + \int_0^\infty U(r') \chi(l, k, r') \phi(l, k, r') dr' \tag{3.3.10}$$

$$f_0(l, k) = \frac{2}{\pi^{\frac{1}{2}}} \Gamma(l + \frac{3}{2}) \left(\frac{k}{2}\right)^{-l} e^{-\frac{1}{2}i\pi l} \tag{3.3.11}$$

Hence as $r \rightarrow \infty$

$$\phi(l, k, r) \rightarrow \frac{1}{2ik} (f(l, k) e^{ikr} - f(l, -k) e^{-ikr}) \tag{3.3.12}$$

But the partial-wave S -matrix is $S(l, k) = e^{2i\delta_l(k)}$, where $\delta_l(k)$ is the phase shift (see (2.2.10)), and is related to the asymptotic form of the regular solution by

$$\phi(l, k, r) \sim (e^{-ikr} - e^{-i(\pi l - kr)}) S(l, k) \tag{3.3.13}$$

i.e. $S(l, k)$ gives the ratio of the outgoing flux ($\chi \sim e^{ikr}$) to the incoming flux ($\chi \sim e^{-ikr}$) for the given partial wave, So in terms of the Jost functions

$$S(l, k) = \frac{f(l, k)}{f(l, -k)} e^{i\pi l} \tag{3.3.14}$$

and the partial-wave scattering amplitude is obtained from this S -matrix by

$$A_l(k) = \frac{S(l, k) - 1}{2ik} \tag{3.3.15}$$

(See (2.2.10). With non-relativistic kinematics $\rho(s) \rightarrow k$.)

b. Analyticity properties of the solutions

The analyticity properties of $A_l(k)$ are readily deduced from those of $f(l, k)$ obtained from (3.3.10).

Poincaré's theorem (Poincaré 1884) states that if a given parameter occurs in a differential equation only in functions which are holomorphic in that parameter, and if the boundary conditions are independent of the parameter, then the solutions to the equation will be holomorphic in the given parameter.

Thus since (3.3.3) is analytic in l , and since if we consider the function $r^{-l-1}\phi(l, k, r)$ the boundary conditions become independent of l , the regular solution $\phi(l, k, r)$ must be analytic in l for $\text{Re}\{l\} > -\frac{1}{2}$. However, for $\text{Re}\{l\} < -\frac{1}{2}$ the regular solution $\rightarrow \infty$ as $r \rightarrow 0$, because $r = 0$ is not a regular point of (3.3.3).

To continue to $\text{Re}\{l\} < -\frac{1}{2}$ we have to analytically continue the integral equation (3.3.4), and the possibility of doing this depends on the nature of the potential. If the potential is singular, i.e. $rU(r) \rightarrow \infty$ for $r \rightarrow 0$, then for a repulsive potential the boundary condition becomes independent of l , since the potential provides the most singular term. So we can simply use the symmetry of (3.3.3) under $l \rightarrow -(l+1)$ to obtain the S -matrix for $\text{Re}\{l\} < -\frac{1}{2}$, i.e. from (3.3.14)

$$S(l, k) = -e^{-2\pi il} S(-l-1, k) \tag{3.3.16}$$

This exhibits the Mandelstam symmetry (2.9.5). However, for an attractive singular potential the S -matrix cannot be defined as there will be an infinite number of bound states (see Frank, Land and Spector 1971).

But we are mainly concerned with potentials which are regular at the origin, like the generalized Yukawa potential (1.13.17). For such we can make the expansions

$$\left. \begin{aligned} rU(r) - k^2 r &= \sum_{n=0}^{\infty} a_n r^n \\ \phi(l, k, r) &= r^{l+1} \sum_{n=0}^{\infty} b_n r^n \end{aligned} \right\} \tag{3.3.17}$$

and on substituting in (3.3.3), and equating coefficients of the various powers of r , one finds

$$\left. \begin{aligned} b_n &= \frac{1}{(2l+n+1)n} \sum_{m=0}^{n-1} a_m b_{n-1-m}, \quad n \geq 1 \\ b_0 &= 1 \end{aligned} \right\} \tag{3.3.18}$$

So ϕ is meromorphic in l with poles at $2l = -(n+1)$, i.e. $2l =$ negative integers, provided that the series (3.3.17) converges for r near zero. The same will be true of the Jost functions in (3.3.9) except that the poles at half-integer l values vanish due to the Mandelstam symmetry.

And since the positions of the poles at negative integer l are independent of r , these fixed poles will cancel in the ratio (3.3.14), and so will be absent from the S -matrix.

If the potential vanishes at the origin, so that $rU(r) \sim r^{p+1}$, which in (1.13.17) implies (expanding the exponential) that

$$\int_m^\infty \rho(\mu)\mu^n d\mu = 0 \quad \text{for } n = 0, 1, \dots, p, \tag{3.3.19}$$

then there are no poles of ϕ_l for integer $\text{Re}\{l\} > -1 - p/2$.

A special intermediate case is potentials which contain a singular term V_0/r^2 . This may be combined with the centrifugal barrier term in (3.3.3) to give an effective angular momentum L , where

$$L(L+1) \equiv l(l+1) + V_0.$$

Thus the poles in L at $L = n$ give rise to branch points in l at

$$l = \frac{1}{2}\{-1 \pm [1 - 4V_0 + 4n(n+1)]\}^{\frac{1}{2}} \tag{3.3.20}$$

whose positions depend on V_0 .

In strong interactions the very-short-distance behaviour of the interaction is the part we know least well, and so the applicability of the above analysis is uncertain. But the fact that the Yukawa potential and its generalizations, which are so analogous to particle exchange forces, do give rise to meromorphic Jost functions for $\text{Re}\{l\} > -1$ suggests that the same may be true in particle physics too.

By precisely similar arguments to the above it can be shown that $\phi(l, k, r)$ is also holomorphic in k for all k ($\text{Re } l > -\frac{1}{2}$), since k appears analytically in (3.3.3) and does not affect the boundary conditions. Similarly $\chi(l, k, r) e^{ikr}$ is holomorphic in k for $\text{Re}\{k\} > 0, \text{Im}\{k\} < 0$. But at $k = 0$ χ has a branch point which can be seen directly in the expression (3.3.8) for χ_0 . The solution for $\text{Re}\{k\} < 0$ can be obtained by continuing round this singularity replacing χ by $\chi(l, k e^{-i\pi}, r)$. Continuation to $\text{Im}\{k\} > 0$ can be achieved by series methods, and it is found that the Jost functions have the Hermitian analyticity property

$$f(l, k) = f^*(l^*, k^*) \tag{3.3.21}$$

However if the potential has the Yukawa form, say, and behaves like e^{-mr} as $r \rightarrow \infty$, then the asymptotic form of the outgoing wave function $\chi \sim e^{ikr}$ is damped away faster than $U(r) e^{-ikr}$ as $r \rightarrow \infty$ if $\text{Im}\{k\} > m/2$ and the series solution breaks down at this point. This is because the partial-wave amplitude has a left-hand cut in k^2 beginning at

$k^2 = -m^2/4$, as one would expect from the analyticity properties discussed in sections 1.13 and 2.6.

Having obtained the singularities of the Jost functions in k and l we can now discuss those of the scattering amplitude, which from (3.3.14) and (3.3.15) may be written

$$A_l(k) = \frac{1}{2ik} \left[\frac{e^{i\pi l} f(l, k) - f(l, -k)}{f(l, -k)} \right] \quad (3.3.22)$$

Clearly its singularities in k^2 will be the same as those of the f 's, namely a left-hand cut starting at $k^2 = -m^2/4$, and a right-hand cut along the positive k^2 axis starting at $k^2 = 0$, as we found in section 1.13. In fact these partial-wave methods can be used to prove that Yukawa potential scattering satisfies the Mandelstam representation (Blankenbecler *et al.* 1960). The right-hand cut is of course a consequence of the unitarity condition $SS^* = 1$, and for integral l , from (3.3.15) and (3.3.21), this becomes

$$A_l(k_+) - A_l(k_-) = 2ikA_l(k_+)A_l(k_-) \quad (3.3.23)$$

where $k_{+,-}$ are evaluated above and below the cut (cf. (2.2.7)). But for non-integral l it is necessary to take out the threshold behaviour first (as in (2.6.8)) so we define

$$B_l(k) = \frac{A_l(k)}{k^{2l}} \quad (3.3.24)$$

which is Hermitian analytic and along the right-hand cut, $k^2 > 0$, satisfies the unitarity equation

$$\begin{aligned} 2i \operatorname{Im} \{B_l(k)\} &\equiv B_l(k_+) - B_l(k_-) = 2ik^{2l+1} B_l(k_+) B_l(k_-) \\ &= 2ik^{2l+1} |B_l(k)|^2 \end{aligned} \quad (3.3.25)$$

(cf. (2.6.23)).

c. Regge poles

In addition to these branch points there is the possibility that pole singularities may appear in (3.3.22) due to the vanishing of $f(l, -k)$. If this happens for a given l at say $k = ik_b$, $k_b > 0$, then it is evident from (3.3.12) that as $r \rightarrow \infty$ the wave function is damped exponentially like $e^{-k_b r}$, corresponding to a bound-state pole on the real negative k^2 axis. Since f is an analytic function of l the position of this pole at $l = \alpha(k_b^2)$, say, where the function α is defined by

$$f(\alpha(k_b^2), -k_b) = 0, \quad (3.3.26)$$

will also be an analytic function of l . On the other hand if there is a zero of $f(l, -k)$ at some $\text{Im}\{k\} < 0$, say $k = k_R - ik_I$, we may write, in this neighbourhood of k ,

$$f(l, -k) \approx C(k - k_R + ik_I)$$

so
$$f(l, k) = f^*(l^*, -k^*) = C^*(k - k_R - ik_I) \tag{3.3.27}$$

where C is some constant, producing a resonance pole in the S -matrix (3.3.14) of the form

$$S(l, k) \approx e^{i(\pi l - 2 \arg C)} \left(\frac{k - k_R - ik_I}{k - k_R + ik_I} \right) \tag{3.3.28}$$

(Note that we cannot have $k_I = 0$ since then both $f(l, k)$ and $f(l, -k)$ would vanish at the same place and so ϕ would vanish.) So resonances will also lie on Regge trajectories, like bound states.

To find the Regge trajectories produced by a given potential one must search for the zeros of $f(l, -k)$. One potential which has particularly simple trajectories is the Coulomb potential $V(r) = e^2/r$. Though this violates the convergence requirements as $r \rightarrow \infty$ ($rU(r) \nrightarrow 0$), it is well known (see for example Schiff (1968) p. 138) that the phase shift $\delta_l(k)$ can still be defined if one first removes the infinite part $\exp[(ie^2 \log r)/2k]$ stemming from the infinite range of the interaction. The S -matrix is then (Singh 1962)

$$S(l, k) = \frac{\Gamma(l + 1 - ie^2/2k)}{\Gamma(l + 1 + ie^2/2k)} \tag{3.3.29}$$

This has poles where the argument of the numerator Γ -function passes through negative integers, i.e. at

$$l = \alpha_n(s) \equiv -m - 1 + \frac{ie^2}{2k}, \quad m = 0, 1, 2, \dots \tag{3.3.30}$$

giving bound states at

$$s = E = k^2 = -\frac{e^4}{4(l + m + 1)^2} \tag{3.3.31}$$

which is the usual Rydberg formula for the hydrogen atom (see fig. 3.1). Note how the trajectories tend to infinity at $E = 0$, which is a characteristic of the zero-mass photon exchange.

With Yukawa-like potentials the Schroedinger equation can be solved numerically using the series method (3.3.17) and some examples are shown in fig. 3.2. A sufficiently attractive potential will produce a bound state for low l , which will become less bound as l increases due to the centrifugal repulsion, and perhaps manifest itself as a higher

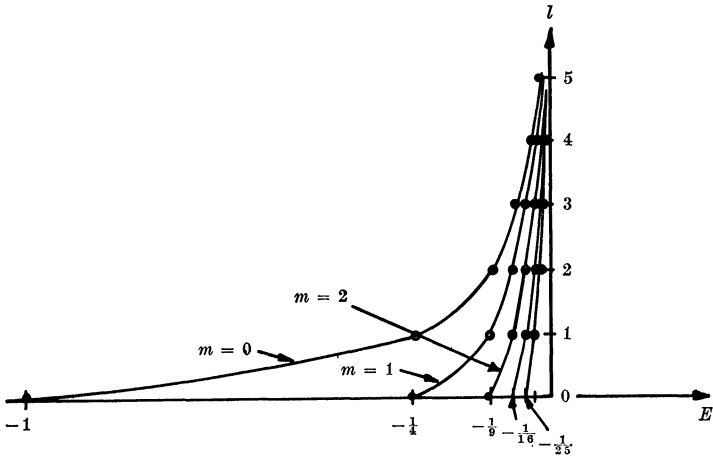


FIG. 3.1 Regge trajectories for the Coulomb potential from (3.2.29). For integer l we have the degenerate hydrogen-atom levels of principle quantum number $n = l + m + 1$ ($m = 0, 1, 2$), where m is the radial quantum number. (E is measured in units of $e^4/4 = 1$ rydberg.)

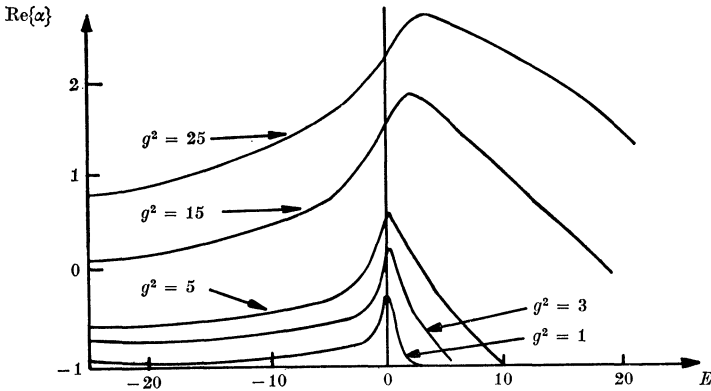


FIG. 3.2 Regge trajectories for an attractive Yukawa potential

$$V(r) = -g^2 e^{-r}/r$$

for various values of g^2 , from Lovelace and Masson (1962). See also Ahmadzadeh, Burke and Tate (1963).

spin resonance. The trajectory turns down again once the effective potential, $U(r) - l(l+1)r^{-2}$, becomes too weak to produce a pole for the given l value. It will also be seen that as $g^2 \rightarrow 0$ the leading trajectory remains near $l = -1$ for all k , i.e. near the position of the highest fixed pole in the Jost function. This is because the Born approximation (1.13.16) or (1.13.18), which behaves like t^{-1} for all s , is a good approximation to the scattering amplitude in this limit.

In fact the leading trajectory asymptotes to -1 for $s \rightarrow \pm \infty$ even for large g^2 because the first Born approximation dominates for large s . However, if the potential vanishes at the origin, $rU(r) \sim r^{p+1}$ as $r \rightarrow 0$, then the trajectory asymptotes to the highest integer $l \leq -1 - (p+1)/2$. This follows from (1.13.18) since if the denominator is expanded for large t

$$A^B(s, t) = - \int_m^\infty d\mu \rho(\mu) \left(\frac{1}{t} + \frac{\mu^2}{t^2} + \dots \right) \tag{3.3.32}$$

it is clear from (3.3.19) that coefficients of $t^{-1}, t^{-2}, \dots, t^{-\frac{1}{2}p-1}$ all vanish.

Other potentials for which the trajectories have been calculated include the square well (see Newton 1964) and the three-dimensional harmonic oscillator, $V(r) = \frac{1}{2}M\omega^2r^2$, where ω is the classical frequency. The eigenstates are (Morse and Feshbach (1953) p. 1662)

$$E = k^2 = \hbar\omega(n + \frac{1}{2}) = \hbar\omega(2m + l + \frac{3}{2}) \tag{3.3.33}$$

giving trajectories with $l \propto E$. This is particularly interesting because with relativistic kinematics $E^2 = k^2 + m^2$ one might expect to get $l \propto E^2$ instead, which corresponds to the behaviour found in particle physics (see chapter 5). Various quark models for meson trajectories have been proposed based on this observation (see Dalitz (1965), and chapter 5) using a static version of the relativistic Bethe–Salpeter equations (see (3.4.11) below) instead of the Schroedinger equation, with a harmonic oscillator potential between the quarks. However, such potentials do not satisfy the convergence requirement that $rV(r) \rightarrow 0$ as $r \rightarrow \infty$ so there are no quark–quark scattering solutions. The quarks can never get out of the potential which, since they have not been observed, may not be a bad thing!

For well behaved potentials it is possible to determine the slope of the trajectory below threshold from the ‘size’ of the bound state. The Schroedinger equation (3.3.3) may be written

$$D\phi = 0 \quad \text{where} \quad D \equiv \left(\frac{d^2}{dr^2} + E - \frac{l(l+1)}{r^2} - U(r) \right) \tag{3.3.34}$$

We seek a solution $\phi(l, k, r)$ for $l = \alpha(E)$ where $E = k^2$. Differentiating with respect to E gives

$$\frac{dD}{dE} \phi + D \frac{d\phi}{dE} = 0 \quad \text{where} \quad \frac{dD}{dE} = 1 - \frac{2\alpha + 1}{r^2} \frac{d\alpha}{dE} \tag{3.3.35}$$

Multiplying (3.3.34) by $d\phi/dE$ and (3.3.25) by ϕ and subtracting gives

$$\frac{d\phi}{dE} D\phi - \phi D \frac{d\phi}{dE} = \phi \frac{dD}{dE} \phi \tag{3.3.36}$$

$$\text{But} \quad D\phi - \phi D = \frac{d^2}{dr^2} \phi - \phi \frac{d^2}{dr^2} \quad (3.3.37)$$

so the left-hand side of (3.3.36) may be written

$$\frac{d}{dr} \left[\frac{d\phi}{dE} \frac{d\phi}{dr} - \phi \frac{d^2\phi}{dE dr} \right] \quad (3.3.38)$$

and integrating both sides from $r = 0$ to ∞ we get

$$\left[\frac{d\phi}{dE} \frac{d\phi}{dr} - \phi \frac{d^2\phi}{dE dr} \right]_0^\infty = \int_0^\infty \frac{dD}{dE} \phi^2 dr \quad (3.3.39)$$

Since $\phi \sim r^{l+1}$ for $r \rightarrow 0$ and $\sim e^{-|k|r}$ for $r \rightarrow \infty$ (for a bound state) the left-hand side vanishes at both limits for $l > -\frac{1}{2}$ and $E < 0$. Then substituting (3.3.35) in the right-hand side of (3.3.39) we end up with

$$\frac{d\alpha}{dE} = \frac{1}{2\alpha + 1} \frac{\int_0^\infty \phi^2 dr}{\int_0^\infty (1/r^2) \phi^2 dr} \equiv \frac{R^2}{2\alpha + 1} > 0 \quad (3.3.40)$$

where R^2 defined by (3.3.40) is the mean-square radius of the state described by the wave function ϕ . It shows that $d\alpha/dE$ is positive for $\alpha > -\frac{1}{2}$, $E < 0$.

d. The N/D method

In obtaining the scattering amplitude from the potential one is seeking a function whose left-hand cut in $E = k^2$ is given by the potential, and whose right-hand cut satisfies the unitarity condition (3.3.25). An alternative to solving the Schrodinger equation which exploits these analyticity properties is the so-called N/D method (Blankenbecler *et al.* 1960). This is of some interest because, unlike the Schrodinger equation, it is readily generalized to particle physics provided the scattering amplitudes have the expected analyticity properties.

From (3.3.22) and (3.3.24) we can write

$$B_l(E) = \frac{f(l, k) e^{i\pi l} - f(l, -k)}{2(ik)^{l+1}} \cdot \frac{1}{(-ik)^l f(l, -k)} \equiv \frac{N_l(E)}{D_l(E)} \quad (3.3.41)$$

Now from (3.3.21) we find that $N_l(k) = N_l(ke^{-i\pi})$ (for real l) so that $N_l(E)$ has no right-hand cut in E but just the left-hand cut stemming from the potential beginning at $E = -m^2/4$, and $N \rightarrow 0$ as $|E| \rightarrow \infty$.

Similarly $D_l(E)$ has no left-hand cut, but just the right-hand unitarity cut, and $D_l(E) \rightarrow 1$ as $|E| \rightarrow \infty$. Both N and D are real analytic.

Hence we can write dispersion relations

$$N_l(E) = \frac{1}{\pi} \int_{-\infty}^{-m^2/4} \frac{\text{Im}\{N_l(E')\}}{E' - E} dE' \tag{3.3.42}$$

$$D_l(E) = 1 + \frac{1}{\pi} \int_0^{\infty} \frac{\text{Im}\{D_l(E')\}}{E' - E} dE' \tag{3.3.43}$$

If we define the discontinuity of $B_l(E)$ across the left-hand cut as $b_l(E)$ we have

$$\text{Im}\{N_l(E)\} = D_l(E) b_l(E), \quad E < -\frac{m^2}{4} \tag{3.3.44}$$

while on the right-hand cut

$$\text{Im}\{D_l(E)\} = N_l(E) \text{Im}\left\{\frac{1}{B_l(E)}\right\} = -N_l(E) \frac{\text{Im}\{B_l(E)\}}{|B_l(E)|^2} = -N_l(E) k^{2l+1} \tag{3.3.45}$$

from (3.3.25), and hence we obtain the simultaneous equations

$$N_l(E) = \frac{1}{\pi} \int_{-\infty}^{-m^2/4} \frac{D_l(E') b_l(E')}{E' - E} dE' \tag{3.3.46}$$

$$D_l(E) = 1 - \frac{1}{\pi} \int_0^{\infty} \frac{N_l(E') E'^{l+\frac{1}{2}}}{E' - E} dE' \tag{3.3.47}$$

The solution of these equations, given $b_l(E)$, corresponds to the solution of the Schroedinger equation with the given potential. The problem of course is to find $b_l(E)$. This is easy for the first Born approximation (1.13.16) whose t -discontinuity is just

$$D_l(E, t) = \pi g^2 \delta(t - \mu^2)$$

which substituted in (2.6.19) (interchanging s and t and putting $q = k$) gives

$$b_l^1(E) = \frac{g^2}{64} P_l \left(1 + \frac{\mu^2}{2k^2}\right) \frac{1}{k^{2l+2}}, \quad E < -\frac{\mu^2}{4} \tag{3.3.48}$$

If this is substituted in (3.3.46) and (3.3.47) we get quite a good approximation to the exact solution for small g^2 . The second Born approximation can also be calculated fairly easily (see Collins and Johnson 1968), but higher order terms are more difficult.

The Regge poles appear as zeros of the D function, i.e. $D_{\alpha(E)}(E) = 0$ implicitly defines $\alpha(E)$, and so a trajectory $\alpha(E)$ can be followed by

observing the movement of this zero with l . This tells us that $\alpha(E)$ will have just the singularities of $D_l(E)$, i.e. just the right-hand cut, in agreement with our conclusions of the previous section.

3.4 Regge poles in perturbation field theory

It is important to check that Regge singularities also occur in perturbation field theory, because this has a much more realistic singularity structure in s and t than potential scattering. We shall find in chapter 8 that more complicated l -plane singularities, Regge cuts, which are absent from potential scattering, also arise in such field theories. But in this chapter we restrict our attention to the poles.

Perhaps the first thing to note is that the theory will include not only Regge poles but also the input elementary particles which correspond to Kronecker- δ functions in the l plane. We are concerned only with scalar mesons, and the partial-wave projection of a t -channel propagator like (1.12.1) is, from (2.2.18) and (A.20),

$$A_l(t) = \frac{g^2}{16\pi} \frac{1}{t - m^2} \delta_{l0} \quad (3.4.1)$$

that is a contribution to the S wave only. Such elementary particles do not seem to exist so we can be fairly sure from the beginning that not all aspects of the l -plane structure of the field theory will correspond to that of particle physics. (However we shall show in chapter 12 that in some circumstances these input δ 's may be cancelled away.) We shall only be interested in the composite particles which may arise as bound or resonant states formed by the interaction between the elementary particles. These should occur on trajectories in analogy with potential scattering.

Such composite particles involve infinite sets of Feynman diagrams, and we shall have to assume that the asymptotic behaviour of such sets of diagrams can be obtained by summing the leading behaviours of the individual diagrams. This certainly need not be true mathematically, of course, but, at least for weak couplings where the perturbation series may make some sense, it has a certain plausibility.

A much more complete review of this subject may be found in Eden *et al.* (1966, chapter 3). Here we are mainly concerned to obtain (3.4.11) below.

For a general Feynman integral like (1.12.5), with n internal lines

and l closed loops, conservation of four-momentum at each vertex can be used to express all the q_i in terms of the loop momenta k_i and the external momenta p_j . Then after judicious changes of variables $k_i \rightarrow k'_i$ the denominator can be rearranged so that the k' integrations can be performed using

$$\int d^4k' \frac{1}{(k'^2 + U)^3} = \frac{i\pi^2}{2U} \tag{3.4.2}$$

and its derivatives with respect to U , and (see Eden *et al.* 1966) one ends up with

$$A = \frac{\int_0^1 \prod_{i=1}^n d\alpha_i \delta(1 - \sum \alpha_i) C(\alpha)^{n-2l-2}}{(D(p, \alpha) + i\epsilon C(\alpha))^{n-2l}} \tag{3.4.3}$$

where D is a function of the p 's and α 's and C a function of the α 's only. Thus for the $2 \rightarrow 2$ scattering amplitude where there are just the two independent invariants s and t and D is linear in s we can rewrite this (dropping the $i\epsilon$ term) as

$$A = \frac{\int_0^1 \prod_{i=1}^n d\alpha_i \delta(1 - \sum \alpha_i) C(\alpha)^{n-2l-2}}{(g(\alpha)s + d(t, \alpha))^{n-2l}} \tag{3.4.4}$$

where g and d are some functions. We are interested in the limit $s \rightarrow \infty$, t fixed, and clearly the integrand $\sim s^{-n+2l}$ unless $g(\alpha) = 0$. So this will also be the behaviour of the integral unless somewhere on the contour of integration $g(\alpha) = 0$, and it is impossible to distort the contour round this point because either (i) $g(\alpha) = 0$ at one of the end points of integration (giving a so-called 'end-point' contribution) or (ii) the point $g(\alpha) = 0$ is 'pinched' by two or more singularities of the integrand as $s \rightarrow \infty$ (see section 1.12).

It can be shown that as long as we stick to just planar diagrams (i.e. diagrams which can be drawn on a sheet of paper without any lines crossing) there will be no pinch contributions on the physical sheet. We shall have to consider non-planar diagrams in chapter 8, but here we shall only be concerned with the end-point contributions of planar diagrams.

Obviously the pole diagram, fig. 3.3 (a), gives

$$A_1 = \frac{g^2}{m^2 - s} \sim \frac{1}{s} \tag{3.4.5}$$

which is just the Born approximation for the t -channel scattering

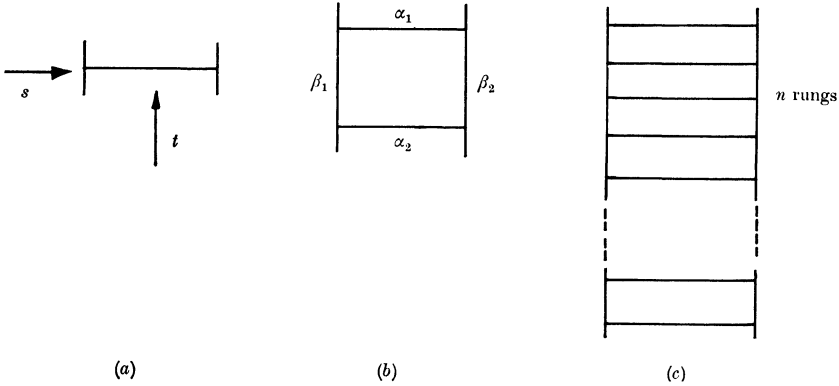


FIG. 3.3 A sequence of *t*-channel ladder Feynman diagrams: (a) the single particle exchange Born approximation, (b) the box diagram with its associated Feynman parameters, (c) an *n*-rung ladder.

process. Then there is the box diagram, fig. 3.3 (b), whose amplitude is

$$A_2 = g^2 \left(-\frac{g^2}{16\pi^2} \right) \frac{\int_0^1 \prod_{i=1}^2 d\alpha_i d\beta_i \delta(1 - \Sigma\alpha_i - \Sigma\beta_i)}{(\alpha_1\alpha_2s + d_2(\alpha, \beta, t))^2} \tag{3.4.6}$$

As $s \rightarrow \infty$ only the behaviour near $\alpha_1, \alpha_2 = 0$ need be considered, and defining $d'_2 = d_2(0, 0, \beta_1, \beta_2, t)$ we need

$$\begin{aligned} \int_0^\epsilon d\alpha_1 d\alpha_2 \frac{1}{(\alpha_1\alpha_2s + d'_2)^2} &= \int_0^\epsilon d\alpha_2 \frac{\epsilon}{d'_2(\epsilon\alpha_2s + d'_2)} \\ &= \frac{1}{d'_2s} \log \left(\frac{\epsilon^2s + d'_2}{d'_2} \right) \sim \frac{\log s}{d'_2s} \end{aligned} \tag{3.4.7}$$

so
$$A_2 \rightarrow g^2 K(t) \frac{\log s}{s} \tag{3.4.8}$$

where
$$\begin{aligned} K(t) &= \frac{-g^2}{16\pi^2} \int_0^1 \frac{d\beta_1 d\beta_2 \delta(1 - \beta_1 - \beta_2)}{d_2(0, 0, \beta_1, \beta_2, t)} \\ &= \frac{g^2}{16\pi^3} \int \frac{d^2\mathbf{K}}{(\mathbf{K}^2 + m^2)[(\mathbf{K} + q)^2 + m^2]}, \quad t = -q^2 \end{aligned} \tag{3.4.9}$$

is the loop integral corresponding to the Feynman diagram fig. 3.4 (a) in which the sides have been contracted out (since $\alpha_1 = \alpha_2 = 0$), which is evaluated only with two-dimensional momentum \mathbf{K} rather than four-dimensional k (because d_2 appears only in the first power, unlike in (3.4.6)).

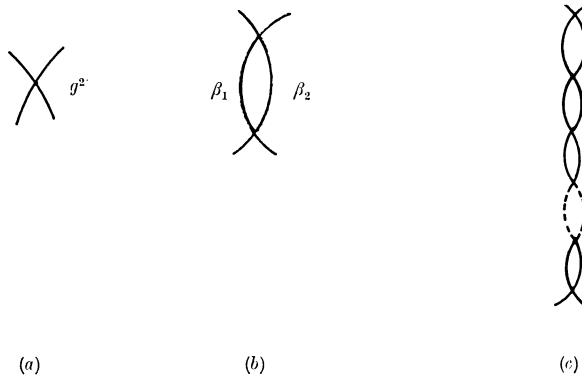


FIG. 3.4 The contracted diagrams corresponding to fig. 3.3 which give the coefficient of the $\sim s^{-1}$ asymptotic behaviour.

For the n -rung ladder diagram, fig. 3.3 (c), it is found similarly that

$$A_n = g^2 \left(\frac{-g^2}{16\pi} \right)^{n-1} (n-1)! \frac{\int_0^1 \prod_{i=1}^n d\alpha_i \pi db \delta(1 - \sum \alpha_i - \sum \beta) C(\alpha, \beta)^{n-2}}{[\alpha_1 \dots \alpha_n s + d_n(\alpha, \beta, t)]^n} \tag{3.4.10}$$

and again, since the leading behaviour comes from the region where the α 's vanish (Fig. 3.4 (b)) the α integrations can be performed to give

$$A_n \sim \frac{g^2 (\log s K(t))^{n-1}}{s (n-1)!} \tag{3.4.11}$$

The power behaviour of all the diagrams in fig. 3.3 is thus s^{-1} like (3.4.5). This is because just a single-particle propagator is needed to get across the diagram. But the power of $\log s$ which appears depends on the number of such propagators.

The next step is to take the asymptotic behaviour of the sum of all such ladder diagrams with any number of rungs, assuming, as mentioned above, that the asymptotic behaviour of the sum is the sum of the asymptotic behaviours. The similarity of figs. 3.3 to figs. 1.14 indicates why this may be rather like solving the Schroedinger equation with a 'potential' given by the Born approximation (3.4.5). From (3.4.11) we get

$$A(s, t) \equiv \sum_n A_n \sim \sum_{n=1}^{\infty} \frac{g^2 (\log s K(t))^{n-1}}{s (n-1)!} \sim \frac{g^2}{s} e^{K(t) \log s} \tag{3.4.12}$$

$$\sim g^2 s^{\alpha(t)} \quad \text{where} \quad \alpha(t) \equiv -1 + K(t) \tag{3.4.13}$$

Clearly, through the Froissart–Gribov projection (2.6.2), the power of

s in (3.4.13) may be identified with the leading t -channel Regge trajectory. Thus we see how the Regge behaviour comes not from any individual diagram, but from the accumulation of $\log s$ powers from the successive interactions of the two particles scattering in the t channel. Since $K(t) \rightarrow 0$ for $t \rightarrow \infty$ (see below) we have $\alpha(t) \xrightarrow[t \rightarrow \infty]{} -1$, due to the behaviour of the Born approximation (3.4.5).

We can check this directly since from (2.3.4) the Born approximation gives

$$A_l^B(t) = \frac{g^2}{32\pi q_t^2} Q_l \left(1 + \frac{m^2}{2q_t^2} \right), \quad q_t^2 = \frac{1}{4}(t - 4m^2) \quad (3.4.14)$$

which from (A.32) has a pole at $l = -1$

$$A_l^B(t) \sim \frac{g^2}{32\pi q_t^2(l+1)} \quad (3.4.15)$$

When this fixed pole is inserted in the unitarity equations it is Reggeized. The partial-wave amplitude must tend to (3.4.14) as $g^2 \rightarrow 0$, and it must satisfy the unitarity equation (2.2.8) which it does if we write it as a series in g^2

$$A_l(t) = \frac{g^2}{32\pi q_t^2} \left[\frac{1}{\alpha(t) - l} - \frac{1}{l+1} \left(1 + \frac{g^2 \alpha_1(t)}{l+1} + \dots \right) \right] \quad (3.4.16)$$

where we have expanded the trajectory function in g^2

$$\alpha(t) = -1 + \frac{g^2}{16\pi} \alpha_1(t) + \dots \quad (3.4.17)$$

and

$$\text{Im} \{ \alpha(t) \} = \frac{g^2}{16\pi q_t \sqrt{t}} \quad (3.4.18)$$

Since $\alpha(t)$ is an analytic function satisfying the dispersion relation (3.2.11) with $n = 1$ we have

$$\alpha(t) = -1 + \frac{g^2}{16\pi^2} \int_{4m^2}^{\infty} \frac{dt'}{q_t' \sqrt{t'}(t'-t)} = -1 + \frac{g^2}{16\pi^2} \frac{1}{q_t \sqrt{t}} \log \left[\frac{2q_t + t^{\frac{1}{2}}}{2q_t - t^{\frac{1}{2}}} \right] \quad (3.4.19)$$

in agreement with (3.4.13). So as expected $\alpha(t) \rightarrow -1$ as $t \rightarrow \pm\infty$ for all g^2 , and for all t as $g^2 \rightarrow 0$. This is almost certainly unrealistic for strong interactions because it stems from the elementary nature of the exchanged scalar meson. But the way in which the trajectory is built up from this basic interaction is so similar to potential scattering that it seems very plausible that a similar mechanism will operate in hadronic physics too. In fact, summing the ladders corresponds to

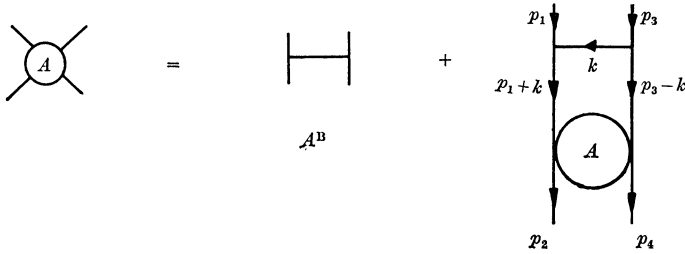


FIG. 3.5 The Bethe–Salpeter equation (3.4.20) for summing ladder diagrams.

solving the *t*-channel Bethe–Salpeter equation (see fig. 3.5) (Bethe and Salpeter 1951, see Polkinghorne, 1964)

$$A(s, t) = A^B(s, t) + \frac{g^2}{(2\pi)^4} \int \frac{d^4k}{[(p_1 + k)^2 - m^2][(p_3 - k)^2 - m^2]} \times A^B(p_1, p_3, p_1 + k, p_3 - k) A(p_1 + k, p_3 - k, p_2, p_4) \quad (3.4.20)$$

which is the relativistic version of the Lippman–Schwinger equation (1.13.27). Trajectories generated by solving the Bethe–Salpeter equation with various potentials have been published by Swift and Tucker (1970, 1971).

3.5 Bootstraps

In section 2.8 we introduced the bootstrap hypothesis that the only set of particles whose existence is compatible with unitarity, analyticity in *s* and *t*, and analyticity in *l*, is the actual set of hadrons found in the real world. If this is so it should be possible to deduce the properties of the particles just by implementing the unitarity equations together with the constraints of crossing. Attempts to achieve this are called ‘bootstrap calculations’.

The complexity of many-body unitarity has made it impossible to test this hypothesis properly so far. We shall examine some of the progress made in this direction in section 11.7, but here we want to illustrate the application of two-body unitarity, to complement our discussion of the previous sections. We review briefly the three main techniques which have been employed.

a. *N/D* equations

These are based on partial-wave dispersion relations, and their development closely parallels the discussion in section 3.3*d*. From

(2.6.20) we can write (Chew and Mandelstam 1960)

$$B_i^{\mathcal{S}}(t) = B_i^L(t) + \frac{1}{\pi} \int_{t_R}^{\infty} \frac{\text{Im}\{B_i^{\mathcal{S}}(t')\}}{t' - t} dt' \tag{3.5.1}$$

where $B_i^L(t)$ is the contribution of the left-hand cut. If we neglect inelasticity completely, so that we can use the elastic unitarity equation (2.6.23) over the whole right-hand cut, this becomes

$$B_i^{\mathcal{S}}(t) = B_i^L(t) + \frac{1}{\pi} \int_{t_R}^{\infty} \frac{\rho_i(t') |B_i^{\mathcal{S}}(t')|^2}{t' - t} dt' \tag{3.5.2}$$

And if we suppose that all the crossed channel singularities are known, i.e. $B_i^L(t)$ is given, then (3.5.2) is an integral equation for the scattering amplitude. To solve it we linearize by writing (cf. (3.3.41))

$$B_i^{\mathcal{S}}(t) = \frac{N_i(t)}{D_i(t)} \tag{3.5.3}$$

where, by definition, the numerator function $N_i(t)$ has the left-hand cut of $B_i^{\mathcal{S}}(t)$, and $D_i(t)$ the right-hand cut. So

$$\text{Im}\{N_i(t)\} = \text{Im}\{B_i^{\mathcal{S}}(t)\} D_i(t) \equiv b_i(t) D_i(t), \quad \text{say, } t < t_L \tag{3.5.4}$$

and

$$\begin{aligned} \text{Im}\{D_i(t)\} &= N_i(t) \text{Im}\left\{\frac{1}{B_i^{\mathcal{S}}(t)}\right\}, \quad t > t_T \\ &= -N_i(t) \frac{\text{Im}\{B_i^{\mathcal{S}}(t)\}}{|B_i^{\mathcal{S}}(t)|^2} = -\rho_i(t) N_i(t) \end{aligned} \tag{3.5.5}$$

from (2.6.23). Since, using (2.2.10) and (2.6.8)

$$\frac{1}{B_i^{\mathcal{S}}(t)} = \frac{D_i(t)}{N_i(t)} = \frac{e^{-i\delta_i(t)}}{\sin \delta_i(t)} \rho_i(t) \tag{3.5.6}$$

and N is real for $t > t_L$, $D_i(t)$ must have the phase $e^{-i\delta_i(t)}$ along the right-hand cut, $t > t_T$.

The Wiener–Hopf method (see Titchmarsh (1937) p. 339) allows one to construct $D_i(t)$ knowing this phase, and the positions of the p_i poles at $t = t_{iu}$, say, and the m_i zeros at $t = t_{ij}$, on the physical sheet. It takes the form

$$D_i(t) = D_i(t_T) \prod_{i=1}^{p_i} \left(\frac{t_T - t_{iu}}{t - t_{iu}}\right) \prod_{j=1}^{m_i} \left(\frac{t - t_{ij}}{t_T - t_{ij}}\right) \exp\left\{-\frac{t - t_T}{\pi} \int_{t_T}^{\infty} \frac{\delta_i(t') - \delta_i(t_T)}{(t' - t)(t' - t_T)} dt'\right\} \tag{3.5.7}$$

We have assumed that $\delta_i(t) \xrightarrow[t \rightarrow \infty]{} \text{constant}$, so that only one subtraction at t_T is needed in the integral. We insist that (as in section 3.3*d*) all

the poles of the amplitude correspond to zeros of $D_l(t)$ (not poles of $N_l(t)$). These may be either bound states on the physical sheet at $t = t_{jl}$, or resonances on unphysical sheets where $\delta_l(t) \rightarrow (2n + 1)\pi/2$.

Then from (3.5.7)
$$D_l(t) \sim t^{\{m_l - p_l + \pi^{-1}[\delta_l(\infty) - \delta_l(t_T)]\}} \tag{3.5.8}$$

We choose conventionally that $D_l(t) \xrightarrow[t \rightarrow \infty]{} 1$ so

$$\delta_l(\infty) - \delta_l(t_T) = \pi[p_l - m_l] \tag{3.5.9}$$

and also that $\delta_l(t_T) = m_l$ giving

$$\delta_l(\infty) = \pi p_l \tag{3.5.10}$$

This relation between the asymptotic value of the phase shift and the number of poles of the D function is known as Levinson’s theorem (Levinson 1949).

From (3.5.5) and (3.5.7) we can write a dispersion relation for $D_l(t)$ in the form

$$D_l(t) = 1 - \frac{1}{\pi} \int_{t_T}^{\infty} \frac{\rho_l(t') N_l(t')}{t' - t} dt' + \sum_{i=1}^{p_l} \frac{\gamma_{ui}}{t - t_{ui}} \tag{3.5.11}$$

where the γ_{ui} are the residues of the poles. Since the γ_{ui} and t_{ui} are arbitrary, $D_l(t)$ is evidently not completely determined by the input $B_l^I(t)$. This is known as the CDD ambiguity, after its discoverers Castillejo, Dalitz and Dyson (1956). An elementary (non-composite) particle like that represented by (3.4.1) would correspond to a CDD pole in the appropriate partial wave.

However for large l the result (2.5.5) implies that $B_l(t) \xrightarrow[l \rightarrow \infty]{} B_l^I(t) \xrightarrow[l \rightarrow \infty]{} 0$

so that $\delta_l(\infty) \rightarrow \delta_l(t_T)$. There will clearly be no bound states in this limit, i.e. $m_l \rightarrow 0$, and hence from (3.5.9) $p_l \rightarrow 0$ too. Thus for large l there is no CDD ambiguity and the scattering amplitudes will be completely determined by $B_l^I(t)$. However, our assumption of analyticity in l requires that the low partial waves should be obtainable from the high partial waves by analytic continuation, and so we cannot just start adding poles in (3.5.11) as l is decreased. So analyticity in l precludes CDD poles in low partial waves as well.

Hence from (3.5.4) and (3.5.5) we arrive at the pair of simultaneous N/D equations

$$N_l(t) = \frac{1}{\pi} \int_{-\infty}^{t_L} \frac{b_l(t') D_l(t')}{t' - t} dt' \tag{3.5.12}$$

$$D_l(t) = 1 - \frac{1}{\pi} \int_{t_T}^{\infty} \frac{\rho_l(t') N_l(t')}{t' - t} dt' \tag{3.5.13}$$

like (3.3.46), (3.3.47). If we introduce the function

$$C_l(t) \equiv N_l(t) - B_l^L(t) D_l(t) \quad (3.5.14)$$

it will have no left-hand cut since

$$\text{Im} \{B_l^L(t)\} = \frac{\text{Im} \{N_l(t)\}}{D_l(t)} \quad (3.5.15)$$

while on the right-hand cut

$$\text{Im} \{C_l(t)\} = -B_l^L(t) \text{Im} \{D_l(t)\} \quad (3.5.16)$$

and so it satisfies the dispersion relation

$$C_l(t) = \frac{1}{\pi} \int_{t_T}^{\infty} \frac{\text{Im} \{C_l(t')\}}{t' - t} dt' \quad (3.5.17)$$

or from (3.5.14)

$$N_l(t) = B_l^L(t) D_l(t) - \frac{1}{\pi} \int_{t_T}^{\infty} \frac{B_l^L(t') \text{Im} \{D_l(t')\}}{t' - t} dt' \quad (3.5.18)$$

Then using (3.5.13) and (3.5.5) to eliminate $D_l(t)$ this becomes

$$N_l(t) = B_l^L(t) + \frac{1}{\pi} \int_{t_T}^{\infty} \frac{B_l^L(t') - B_l^L(t)}{t' - t} \rho_l(t') N_l(t') dt' \quad (3.5.19)$$

This is an integral equation for $N_l(t)$ given $B_l^L(t)$ which can be solved numerically. Once $N_l(t)$ is found it can be substituted in (3.5.13) to find $D_l(t)$.

These equations can be generalized to include inelastic states (for a review see Collins and Squires (1968) chapter 6). The most important change is that it is then possible for bound or resonant states of one channel to appear as CDD poles in another channel. However, such a CDD zero will emerge from the inelastic cut as l is decreased, so continuity in l is not destroyed, and such CDD poles do not correspond to elementary particles.

A zero of $D_l(t)$ at some $t = t_r$, say, corresponds to a pole of the partial-wave amplitude. Continuing the solution in l we generate a trajectory $\alpha(t)$ such that

$$D_{\alpha(t_r)}(t_r) = 0 \quad (3.5.20)$$

Then expanding $D_l(t)$ about $l = \alpha(t_r)$ we have (from (3.5.3))

$$B_l^L(t) \approx \frac{N_{\alpha}(t_r)}{(l - \alpha(t_r)) (\partial D_l / \partial l)_{l=\alpha(t_r)}^{t=t_r}}, \quad l \approx \alpha(t_r), \quad t \approx t_r \quad (3.5.21)$$

so the residue of the Regge pole is given by $N(\partial D / \partial l)^{-1}$.

A simple example of the use of such equations is the ρ bootstrap

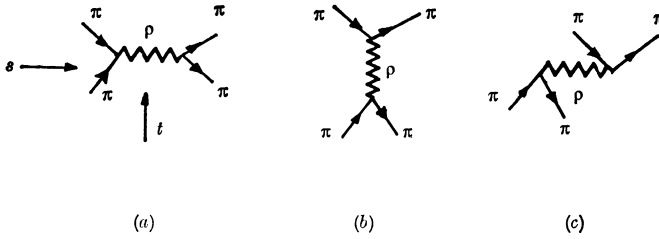


FIG. 3.6 The ρ -exchange poles in the s -, t - and u -channels of $\pi\pi$ scattering.

(Zachariasen 1961, Balazs 1962, 1963, Collins 1966). This is based on the observation that the dominant singularity in low energy elastic $\pi\pi$ scattering is the spin = 1 ρ resonance. Because $\pi\pi$ scattering is crossing symmetric this resonance will occur in all three s , t and u channels (fig. 3.6). So if we make the very drastic approximation that this is the only important singularity we can obtain the left-hand cut of the t -channel partial-wave amplitude from the ρ poles in the s and u channels. Thus from (2.6.14)

$$B_l^I(t) = \frac{g_\rho^2}{16\pi} \frac{q_\rho^2}{q_t^{2l+2}} Q_l \left(1 + \frac{m_\rho^2}{2q_t^2} \right) P_1 \left(1 + \frac{t}{2q_\rho^2} \right) \tag{3.5.22}$$

where

$$q_\rho^2 \equiv \frac{1}{4}(m_\rho^2 - m_\pi^2)$$

The mass of ρ , m_ρ , and its coupling strength to $\pi\pi$, g_ρ , can be regarded as free parameters. Then if we insert (3.5.22) in (3.5.19), solve the equation, and insert the solution for $N_l(t)$ in (3.5.13) we obtain an output t -channel trajectory and residue from (3.5.20) and (3.5.21). Crossing symmetry requires that $D_l(t)$ should have a zero for $l = 1$ at $t = m_\rho^2$, and that the residue should be g_ρ^2 . Hence one can try and adjust these parameters until self-consistency under crossing and unitarity is achieved, and thereby deduce the mass and coupling of the ρ from self-consistency requirements only.

Unfortunately there are several technical problems concerning the divergence of the integral in (3.5.19) which requires a cut-off, but a qualitative success may be claimed (see Collins and Squires (1968) chapter 6). This is probably the most we can expect given that we have neglected all the other singularities and inelastic unitarity. But the most important point is that this method of generating trajectories in particle physics is based on methods which we know can be employed successfully in potential scattering.

b. The Cheng–Sharp method

Another way of using partial-wave unitarity to calculate Regge trajectories was suggested by Cheng and Sharp (1963) and Frautschi, Kaus and Zachariassen (1964).

If the partial-wave amplitude is expressed as a sum of Regge poles plus the background integral

$$B_l^{\mathcal{S}}(t) = \sum_{i=1}^n \frac{\gamma_i(t)}{l - \alpha_i(t)} + \bar{B}_l^{\mathcal{S}}(t) \quad (3.5.23)$$

and substituted in the unitarity equation (2.6.23), or (4.7.4) below, for $l \rightarrow \alpha_j(t)$ we get

$$\frac{1}{2i\rho_{\alpha_j}(t)} = \sum_i \frac{\gamma_i^*(t)}{\alpha_j(t) - \alpha_i^*(t)} + \bar{B}_{\alpha_j^*}^{\mathcal{S}*}(t), \quad \text{for } j = 1, 2, \dots, n \quad (3.5.24)$$

a set of simultaneous equations for the Regge parameters given the background integral (which contains the crossed-channel singularities, i.e. the ‘potential’). If one supposes that just a single pole α_j dominates with $\text{Im}\{\alpha_j\}$ small, then \bar{B} can be neglected and (3.5.24) becomes

$$\text{Im}\{\alpha_j(t)\} = \rho_{\alpha_j}(t) \gamma_j(t), \quad \text{Im}\{\gamma_j(t)\} = 0 \quad (3.5.25)$$

which has the correct threshold behaviour (3.2.26).

To proceed further it is necessary to modify the Regge pole terms so that they have the correct Mandelstam analyticity. (The s discontinuity in (2.8.10) starts at $z_t = -1$, from (A.13), i.e. at $s = -4q_t^2$ for equal-mass kinematics, rather than at the threshold s_T (see Collins and Squires (1968) chapter 3). One must also add the crossed-channel poles, which provide the potential, in $\bar{B}_l^{\mathcal{S}}$. This method has been applied successfully in calculating trajectories in potential-scattering problems (Hankins, Kaus and Pearson 1965), and, with many necessary modifications, for some bootstrap calculations (Abbe *et al.* 1967).

c. The Mandelstam iteration

This method makes direct use of the Mandelstam representation discussed in section 1.11. Elastic unitarity is used to obtain the double spectral functions, ρ_{st} , in those regions of the s – t plane where elastic unitarity holds, and the asymptotic behaviour of ρ_{st} gives the trajectory.

From (1.5.7) the discontinuity across the elastic cut for $t_T < t < t_I$ in the t channel is

$$D_t(s, t) = \frac{q_t}{32\pi^2\sqrt{t}} \int d\Omega_t A^+(s', t) A^-(s'', t) \tag{3.5.26}$$

where (see (2.2.3) with $s \leftrightarrow t$) $s' = s(z', t)$, $z' \equiv \cos \theta_{in}$ being the cosine of the scattering angle between the direction of motion of the particles in the initial and intermediate states, and where $s'' = s(z'', t)$ and $z'' \equiv \cos \theta_{nf}$, the cosine of the angle between the intermediate and final states, in the t -channel centre-of-mass system. Similarly $s = s(z_t, t)$ where $z_t = \cos \theta_{if}$ (see fig. 2.1) and $d\Omega_t \equiv dz'' d\phi$. These angles are related by the addition theorem (2.2.4), i.e.

$$z' = z_t z'' + \sqrt{(1 - z_t^2)} \sqrt{(1 - z''^2)} \cos \phi \tag{3.5.27}$$

Formally we can substitute the dispersion relation (1.10.7) for A^+ and A^- into (3.5.26) and obtain at fixed t (neglecting the pole terms for simplicity)

$$D_t(s, t) = \frac{q_t}{32\pi^2\sqrt{t}} \int d\Omega_t \left[\frac{1}{\pi} \int_{s_T}^{\infty} \frac{D_s(s_1, t_+)}{s_1 - s'} ds_1 + \frac{1}{\pi} \int_{u_T}^{\infty} \frac{D_u(u_1, t_+)}{u_1 - u'} du_1 \right] \\ \times \left[\frac{1}{\pi} \int_{s_T}^{\infty} \frac{D_s(s_2, t_-)}{s_2 - s''} ds_2 + \frac{1}{\pi} \int_{u_T}^{\infty} \frac{D_u(u_2, t_-)}{u_2 - u''} du_2 \right] \tag{3.5.28}$$

with (from (1.7.21))

$$s + t + u = s' + t + u' = s'' + t + u'' = s_1 + t + u_1 = s_2 + t + u_2 = \Sigma \tag{3.5.29}$$

If then we replace the s 's and u 's by z 's using (2.3.2) and change the order of integration we find terms of the form

$$\int_{-1}^1 dz'' \int_0^{2\pi} d\phi \frac{1}{(z_1 - z')(z_2 - z'')} = \frac{2\pi}{\Delta^{\frac{1}{2}}} \log \left(\frac{z - z_1 z_2 + \Delta^{\frac{1}{2}}}{z - z_1 z_2 - \Delta^{\frac{1}{2}}} \right) \tag{3.5.30}$$

using (3.5.27), where

$$\Delta(z_t, z_1, z_2) \equiv -1 + z_t^2 + z_1^2 + z_2^2 - 2z_t z_1 z_2 \tag{3.5.31}$$

and we must take the branch of the logarithm which is real for $-1 < z < 1$. So converting back from z 's to s 's we get

$$D_t(s, t) = \frac{q_t}{16\pi^3\sqrt{t}} \int_{s_T}^{\infty} \frac{ds_1}{2q_t^2} \int_{s_T}^{\infty} \frac{ds_2}{2q_t^2} (D_s(s_1, t_+) + D_u(s_1, t_+)) (D_s(s_2, t_-) \\ + D_u(s_2, t_-)) 2q_t^2 K^{-\frac{1}{2}} \log \left(\frac{s - s_1 - s_2 - (s_1 s_2 / 2q_t^2) + K^{\frac{1}{2}}}{s - s_1 - s_2 - (s_1 s_2 / 2q_t^2) - K^{\frac{1}{2}}} \right) \tag{3.5.32}$$

where

$$K(s, s_1, s_2, t) \equiv [s^2 + s_1^2 + s_2^2 - 2(ss_1 + ss_2 + s_1s_2) - ss_1s_2/q_t^2] \quad (3.5.33)$$

Now from (1.11.11) the double spectral function $\rho_{st}(s, t)$ is just the discontinuity of $D_t(s, t)$ across its cuts in s . This discontinuity arises from the vanishing of K . But $K \rightarrow 0$ makes the logarithm tend to $\log 1 = 2\pi ni$, where n depends on the branch of the logarithm which is chosen. So the discontinuity in going round the threshold branch point in s for $K > 0$ is just 2π . Hence

$$\rho_{st}(s, t) = \frac{1}{8\pi^2} \frac{q_t}{\sqrt{t}} \int_{s_T}^{\overbrace{s}^{K=0}} \frac{ds_1}{2q_t^2} \int_{s_T} \frac{ds_2}{2q_t^2} \frac{D_s(s_1, t_+) D_s(s_2, t_-)}{K^{\frac{1}{2}}(s, s_1, s_2, t)} 2q_t^2 \quad (3.5.34)$$

The region of integration is over $s_1, s_2 > s_T$ but with $K > 0$, since there is no discontinuity for $K < 0$. The boundary in s of $\rho_{st}(s, t)$ is given by the lowest values of s_1, s_2 , i.e. where

$$K(s, s_T, s_T, t) = s \left(s - 4s_T - \frac{s_T^2}{q_t^2} \right) = 0 \quad (3.5.35)$$

But $s = 0$ is not a singular point of (3.5.32) so the boundary is

$$s = 4s_T + \frac{s_T^2}{q_t^2} \equiv b(t) \quad (3.5.36)$$

From (1.11.4) we have

$$D_s(s, t) = \frac{1}{\pi} \int_{b(s)}^{\infty} \frac{\rho_{st}(s, t'')}{t'' - t} dt'' + \text{other terms} \quad (3.5.37)$$

The most important ‘other term’ is the s -channel bound-state pole from the Born approximation (2.6.13)

$$D_s^B = \pi g^2 \delta(s - m^2) \quad (3.5.38)$$

If this is substituted in (3.5.34) we get

$$\rho_{st}(s, t) = \frac{g^4}{16q_t(s - 4m^2 - m^4/q_t^2)^{\frac{1}{2}} \sqrt{t} \sqrt{s}} \quad (3.5.39)$$

whose boundary is at $K(s, m^2, m^2, t) = 0$, i.e. (1.12.10). Then if (2.5.39) is substituted into (3.5.37) we get an additional contribution to D_s (over and above (3.5.38)), which may in turn be substituted in (3.5.34) to give a further contribution to $\rho_{st}(s, t)$ with a boundary at $K(s, 4m^2, 4m^2, t) = 0$; and so on. Hence we can find $D_s(s, t)$ by iteration, the successive contributions to the double spectral function having boundaries at higher and higher s , as shown in fig. 3.7. This is just

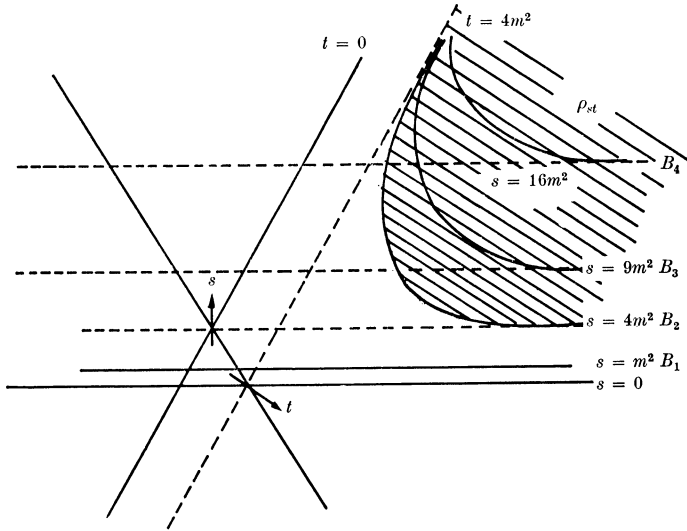


FIG. 3.7 The boundaries of the successive contributions to the double spectral function (B_2, B_3, B_4, \dots) obtained by iterating the input s -channel pole B_1 with t -channel unitarity. The asymptotic s behaviour will be $\rho(s, t) \sim s^{\alpha(t)}$ for fixed t , which enables the trajectory to be found.

another way of summing the ladders corresponding to multiple exchange of the Born approximation (3.5.38). Indeed (3.5.39) gives us the behaviour (3.4.8), and the various iterations agree with (3.4.11).

Of course (3.5.38) is unrealistic as a Born approximation for particle physics. Attempts have been made to incorporate crossing symmetry by taking s -channel Regge poles as the input, and generating t -channel Regge poles as output, and seeking bootstrap self-consistency as described in section 3.5*a*, but so far with only modest success (see Collins and Johnson 1969, Webber 1971). We shall explore other similar dynamical schemes in chapter 11. However, it seems likely that the restriction to just planar diagrams with elastic unitarity precludes a proper self-consistent answer. Our purpose in discussing this method here has been to show that the Mandelstam iteration gives yet another procedure for generating Regge trajectories by summing ladder diagrams.